Pergamon

Cement and Concrete Research, Vol. 25, No. 7, pp. 1581-1590, 1995

0008-8846/95 $9.50+.00

0008-8846(95)00151-4

MICROSTRUCTURAL AND MICROANALYTICAL STUDIES OF SULFATE ATTACK III. SULFATE-RESISTING PORTLAND CEMENT: REACTIONS WITH SODIUM AND MAGNESIUM SULFATE SOLUTIONS

R.S. Gollop and H.F.W. Taylor
Blue Circle Industries PLC
Technical Centre, 305 London Road
Greenhithe, Kent DA9 9JQ, UK

(Refereed)
(Received February 8; in final form April 12, 1995)

ABSTRACT

Cubes of a sulfate-resisting Portland cement (SRPC) paste that had been stored for 6 months in solutions of Na_2SO_4 or $MgSO_4$ were examined by scanning electron microscopy using backscattered electron imaging and X-ray microanalysis. The changes observed were broadly similar to those which we have found with a normal Portland cement (PC), but cracking and loss of material were less marked, less ettringite was formed, and decalcification of the C-S-H was much reduced. As with the PC, gypsum was formed, both in veins and mixed with the C-S-H. The differences are attributed to the low content of Al_2O_3 in the hydration products of the SRPC, and to the fact that some of the Al_2O_3 is already present as ettringite. The decreased formation of ettringite and decreased decalcification of the C-S-H in the SRPC together explain the superior resistance to sulfate attack.

Introduction

It is well established that mortars and concretes made using sulfate-resisting Portland cements (SRPC) resist external sulfate attack better than those made using normal Portland cements (PC; 1–5, etc), but only a few studies appear to have been reported on the chemical or microstructural changes that occur when SRPC pastes react with sulfate solutions. Using X-ray diffraction and differential thermal analysis, Heller and Ben-Yair (6) found that similar quantities of ettringite were formed in pastes of PC and SRPC under comparable conditions, but that expansions were much lower with SRPC. Much more ettringite was formed in a paste exposed to a 10 % sodium sulfate solution than in pastes exposed to weaker solutions, but there was no direct relation between the amount of ettringite formed and the degree of expansion. Locher (7) found that exposure of an SRPC to 4.4 % Na_2SO_4 solution produced gypsum, but only small amounts of ettringite or monosulfate. Dimic and Droljc (8) studied the action of Na_2SO_4 solutions on mortars made from six different SRPCs. With the SRPCs high in C_3S (> 60 % Bogue), attack was more severe than with the others, and substantial quantities of both ettringite and gypsum were found by XRD. With those lower in C_3S, significantly less gypsum was found at the end of the test. In a study of the somewhat similar case of hydration of highly oversulfated cements, Odler and Gasser (9) found that an SRPC yielded less ettringite than did a white cement under comparable conditions, and that for a given quantity of ettringite expansion was less with the SRPC.

Rasheeduzzafar et al. (10) studied the action of a mixed sodium and magnesium sulfate solution on pastes and mortars made with several plain and blended cements, including an SRPC. The SRPC, after being cured for 2 years in water alone, gave an XRD pattern that included a broad peak at 9–10° 2θ (CuKα), which was attributed to ettringite and monosulfate. The pattern obtained after a similar period of curing in the sulfate solution differed in showing less calcium hydroxide and in the presence of strong peaks of gypsum and weaker peaks of brucite. In contrast to what was found with a PC, there was no evidence of any increase in the content of ettringite. SEM observations confirmed that much gypsum had been formed and also showed significant replacement of C-S-H by magnesium silicate hydrate. Studies using a sodium sulfate solution (11) similarly showed the formation of a significant amount of gypsum but only a little ettringite.

In Part I of this series (12), we reported the results of a microstructural and microchemical study of sulfate attack on a paste of a PC (BS12, PC Class 42.5), and in Part II (13) we described the ferrite composition and hydration chemistry of an SRPC . In this paper, we report on a study of sulfate attack on a paste of this SRPC, using the same procedures as for the PC.

Experimental

The chemical analysis and other data for the SRPC (BS4027, SRPC Class 42.5) are given in Ref. 13. Using this cement, cubes were prepared having a water:cement ratio of 0.3 and were stored in 0.25 mol l^{-1} solutions of Na_2SO_4 or $MgSO_4$ at 20°C for 6 months, and were then examined by scanning electron microscopy with backscattered electron (BSE) imaging and X-ray microanalysis. All the experimental techniques were as described in Part I (12). The SEM observations were made on polished sections cut parallel to a cube face; 214 spot analyses of hydrated material were recorded for the cube stored in Na_2SO_4 solution, and 85 for that stored in $MgSO_4$ solution. These numbers do not include analyses made on the unattacked cores of the cubes, which were reported in Part II (13).

The faces of the cubes showed little visible damage, but at the cube edges material had been lost, giving surfaces bevelled by corrosion. The damage at the edges was less pronounced than with the corresponding cubes made using the PC (12).

Results

Cube Stored in Na_2SO_4 Solution

BSE images of a section including a cube face and remote from the cube edges were closely similar to those reported for the PC paste immersed in Na_2SO_4 solution (12). There was, typically, a single band of gypsum 20–25 μm thick and 150 μm beneath the surface with some microcracking largely along the edges of the band. In the outermost 50–100 μm, the paste had the dark appearance characteristic of decalcified material, and the unreacted clinker residues were largely of ferrite; there was no observable $Ca(OH)_2$. These effects diminished with depth and were usually imperceptible at depths greater than about 200 μm. At the cube edges, cracking and loss of material were much less marked than with the PC, and there was only a single gypsum vein sub-parallel to the corroded edge (Fig. 1). This contrasts with the multiple gypsum veins observed in this area in the case of the cube made with PC. Along a line perpendicular to the corroded

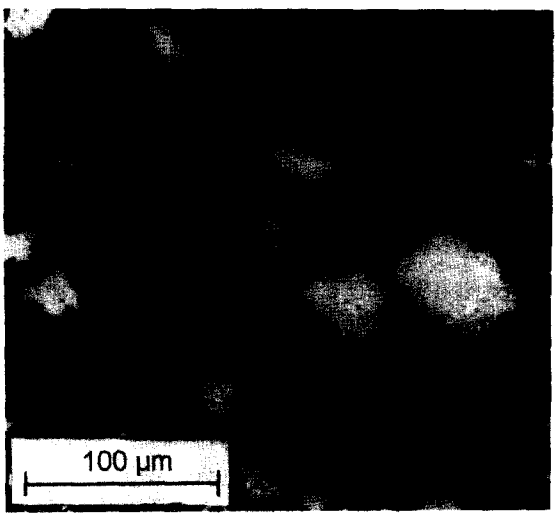

FIG. 1

Backscattered electron image of paste stored in Na_2SO_4 solution; section cut perpendicular to a cube edge just outside the field of view at the top right.

edge, the paste was moderately dark and little or no $Ca(OH)_2$ was detectable to a depth of some 400 μm.

In Fig. 2A, the Si/Ca atom ratios are plotted against depth below the face or edge of the cube. In the unattacked core, the large group of spots with ratios of 0.4–0.5 represents C-S-H gel as defined in Ref. 12, and shown to be probably an intimate mixture of C-S-H with varying small proportions of ettringite and hydrotalcite- and hydrogarnet-type phases (13). Lower ratios represent mixtures in which $Ca(OH)_2$ or, rarely, monosulfate is also present. On moving outwards towards the cube face or edge, the upper limit of Si/Ca ratio increases only slightly until the last 50–100 μm below the external surface, beyond which it increases sharply. Except in this outermost zone, therefore, decalcification is slight.

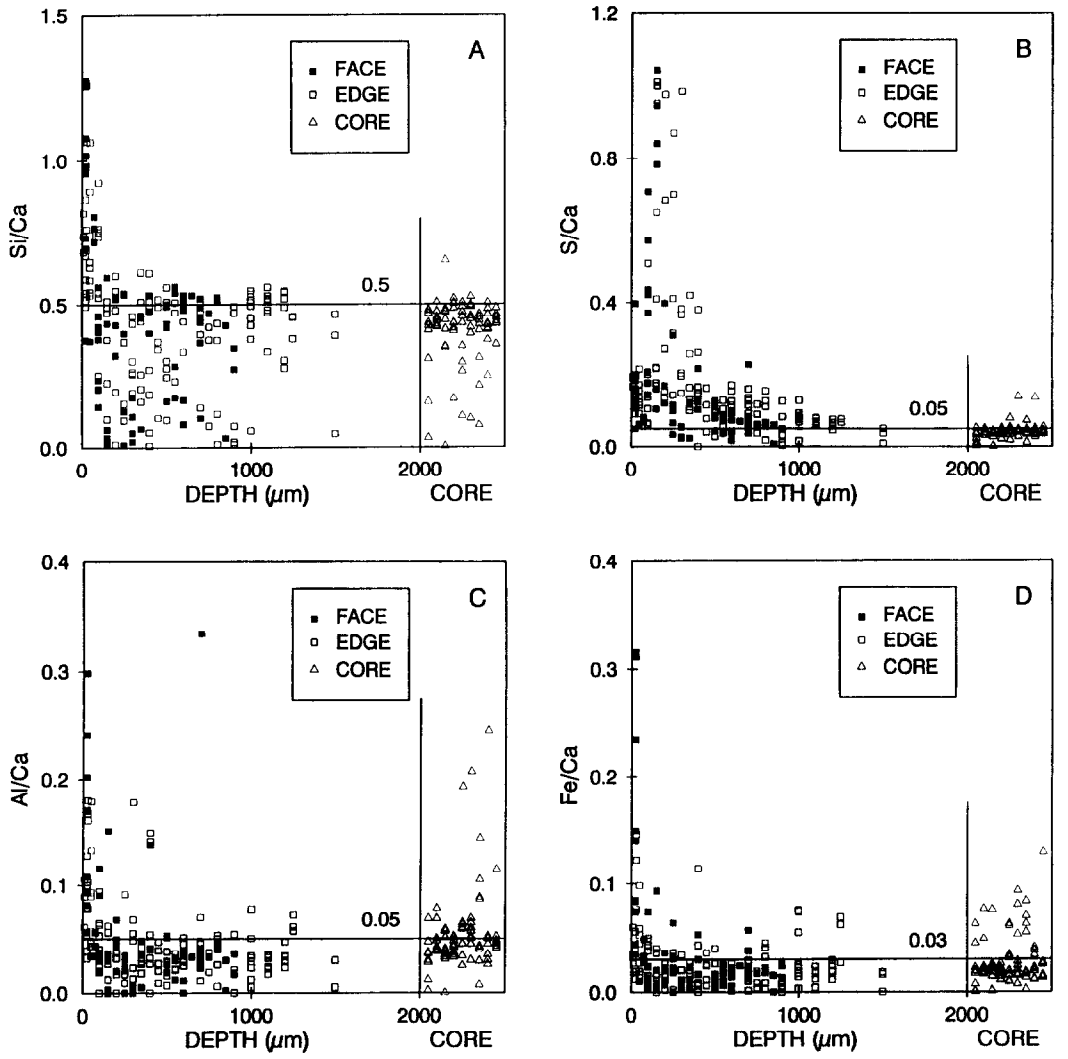

FIG. 2

Plots of atom ratios against depth below the surface for the paste stored in Na_2SO_4 solution. Open squares: spots at given depths measured diagonally from a corroded edge. Filled squares: spots at given depths below a face of the cube, at points remote from an edge. Triangles: spots in the unreacted core of the cube (arbitrarily placed in the direction parallel to the depth axis).

The S/Ca (sulfur/Ca) ratios (Fig. 2B) are mostly below 0.05 in the unattacked core, and on moving outwards increase gradually towards values close to 1.0 in the gypsum vein before falling again as the external surface is approached. Below the cube faces, the sulfate does not appear to have penetrated more deeply than 1000 μm. Below the edges, the penetration is clearly greater, and probably extends to a depth of at least 1250 μm.

Fig. 2C shows Al/Ca ratios. For the core material, the spots with values in the region of 0.05 are of the C-S-H gel as defined above. Lower values represent mixtures of the C-S-H gel with $Ca(OH)_2$, and values higher than about 0.1 represent mixtures containing monosulfate. For the reacted material at depths of 150–1500 μm below either the edge or the face, almost all the spots have Al/Ca ratios below 0.07. This suggests that the monosulfate has reacted to form a product, presumably ettringite, that is more closely mixed with the C-S-H. The high values of the Al/Ca ratio at points close to the surface indicate that decalcification has occurred.

The plot of Fe/Ca ratios against depth (Fig. 2D) broadly resembles that of the Al/Ca ratios. In the core, most of the spots showed ratios of 0.02–0.03 with a scattering of higher values up to 0.13. Relatively few spots in the 150–1500 μm region show ratios higher than 0.03; in this respect, the pattern is analogous to that for Al/Ca. The effect is less marked than in the latter case and may not be statistically significant. The Mg/Ca ratios did not vary significantly with depth, except in the surface region, where they increased due to loss of calcium. Plots of K/Ca or Na/Ca against depth showed no significant trends until close below the surface, where high values were observed. In the last 100 μm, the Na/S ratios clustered around 2.0, showing the presence of Na_2SO_4. This had probably formed by evaporation of absorbed solution during sample preparation.

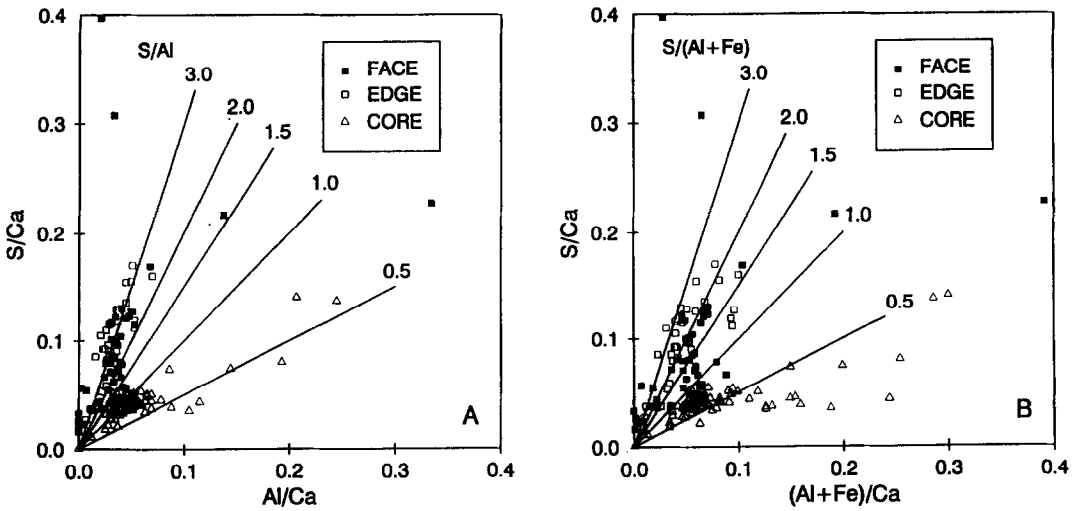

FIG. 3

Atom ratio plots of (A) S/Ca against Al/Ca and (B) S/Ca against (Al + Fe)/Ca, in each case for spots at depths of 200–800 μm below the face, or 500–800 μm below the edge, of the cube stored in Na_2SO_4 solution. Conventions as in Fig. 2; analyses for the core material (triangles) are also included.

In Fig. 3A, S/Ca ratios are plotted against Al/Ca ratios for spots at depths of 500–800 μm beneath the edge and of 200–800 μm below the face. The lower limits were chosen so as to avoid any obvious vein of gypsum. Data for spots in the core are also included. In the latter, the C-S-H gel has a mean S/Al (sulfur/Al) ratio of about 1.0, and there are a number of spots having S/Al ratios in the region of 0.5 and relatively high Al/Ca ratios, which probably contained substantial proportions of monosulfate. In the altered regions, the median S/Al ratio of the C-S-

H gel has increased to around 2.7, and the spots with Al/Ca ratios above 0.07 have almost disappeared, indicating that the monosulfate has reacted. A plot of S/Ca against (Al + Fe)/Ca for the same range of spots (Fig.3B) gave similar results, and indicated a median S/(Al + Fe) ratio in the altered regions of approximately 2.0. A plot of Al/Ca against Si/Ca for the same range of spots gave no useful additional information.

Cube Stored in $MgSO_4$ Solution

BSE images of regions distant from the cube edge were closely similar to those observed with PC (12). They showed a composite band of brucite and gypsum at the surface, with the brucite on the outside and having a total thickness of 50–70 μm. In places, there were surface deposits of $CaCO_3$, which XRD showed to be predominantly aragonite. For a distance of 50–150 μm below the band of brucite and gypsum, the paste had an altered appearance, characterised by darkening of the C-S-H, near absence of residual clinker phases other than ferrite, little or no $Ca(OH)_2$ and irregular microcracking. The BSE images at the cube edges (Fig. 4) were also similar to those observed with the PC. A strongly altered dark and cracked region extended inwards from the corroded edge of the cube to a depth of 500–550 μm, measured along the diagonal. Microanalyses showed that it consisted largely of magnesium silicate hydrate, with minor amounts of other phases. These were mainly ferrite with occasional $CaCO_3$. In a region extending for a further 200 μm along the diagonal, the paste was more nearly normal, but had a somewhat darkened appearance and there were multiple gypsum veins and cracks sub parallel to the edge bevelled by corrosion. Deeper in, there was no apparent alteration.

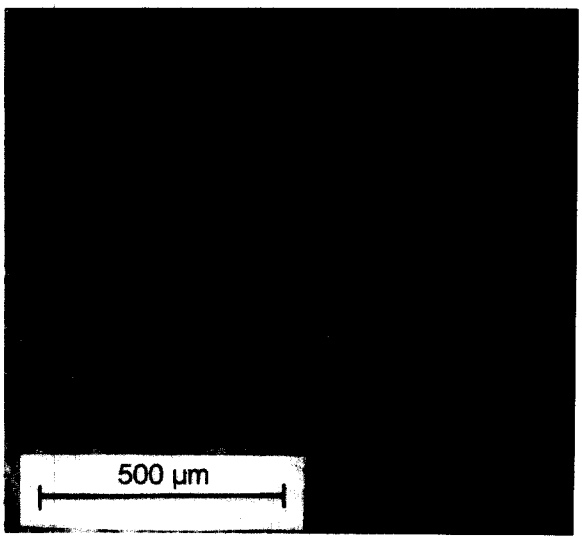

FIG. 4

Backscattered electron image of the paste stored in $MgSO_4$ solution; section cut perpendicular to a cube edge.

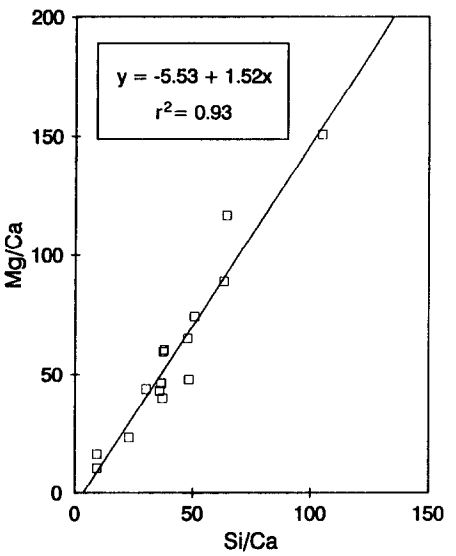

FIG. 5

Atom ratio plot of Mg/Ca against Si/Ca for spots consisting essentially of magnesium silicate hydrate.

In Fig. 5, Mg/Ca ratios are plotted against Si/Ca ratios for all the analyses made in the region consisting essentially of magnesium silicate hydrate. The results show that the Mg/Si ratio is close to 1.5; this supports the characterisation (12) of this material as a poorly crystalline form of serpentine ($M_3S_2H_2$). A plot of log (Mg/Ca) against depth (Fig. 6A) showed that penetration of the Mg^{2+} was, at most, very slight at depths beyond the layer of brucite and gypsum at the cube face or beneath the region of magnesium silicate hydrate at the cube edge. Insufficient

data were obtained to determine the limits of sulfate penetration, but plots of log (S/Al) or log (S/Ca) against depth showed that this was substantial up to depths of at least 500 μm below the cube face or 800 μm below the corroded cube edge.

A plot of log (Si/Ca) against depth (Fig. 6B) showed that, beneath the cube faces, decalcification was almost negligible at depths greater than about 200 μm. This agrees with the conclusions from the BSE image. In the region below the cube edges, the high values of log (Si/Ca) at depths up to 550 μm correspond to spots consisting largely of magnesium silicate hydrate. At greater depths, the analyses indicate moderate degrees of decalcification (Si/Ca up to 0.7). No analyses were made at depths greater than 800 μm, other than those of the core material, but the BSE images indicated that there was little or no decalcification in this region.

Plots of Al/Ca or Fe/Ca against Si/Ca and of S/Ca against Al/Ca for regions not complicated by the presence of obvious gypsum veins or magnesium silicate hydrate gave results similar to those described for the paste stored in sodium sulfate solution.

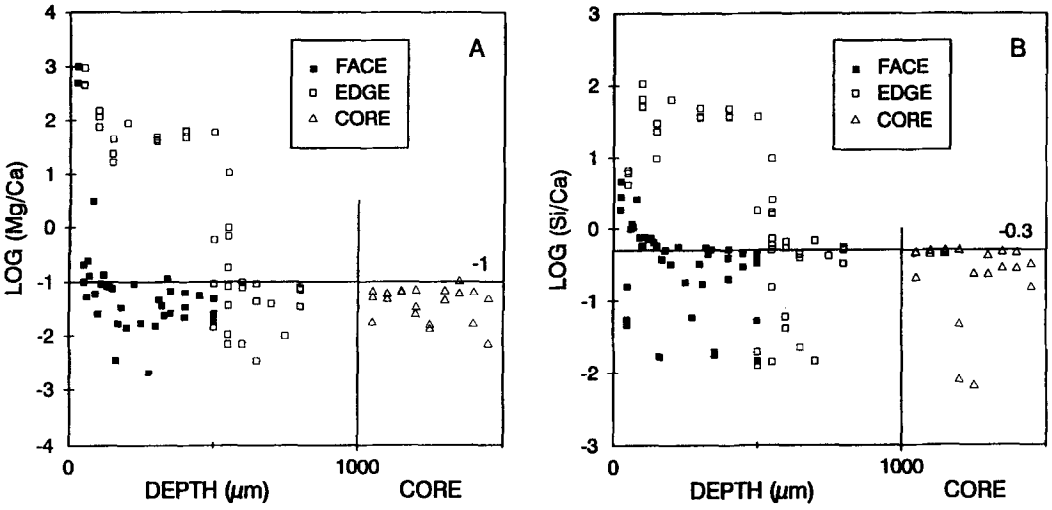

FIG. 6

Atom ratio plots of (A) log (Mg/Ca) and (B) log (Si/Ca) against depth for the paste stored in $MgSO_4$ solution. Conventions as in Fig. 2.

Discussion

Interpretation of X-Ray Microanalyses: Formation of Gypsum and of Ettringite

As we have noted earlier (13), the relation between the S/Al ratio given by an X-ray spot microanalysis and the nature of any hydrated sulfoaluminate phase is less clear cut for an SRPC paste than for a PC paste, because of the low content of Al_2O_3 relative to the other oxide components. In an SRPC paste that has reacted with a sulfate solution, interpretation of the data is further complicated by uncertainties as to the extents to which the various Al- and Fe-containing phases react. Irrespective of the assumptions made, most of the spots represented in Fig. 3A and B, other than those from the core, cannot obviously be explained without postulating the presence of gypsum. On the other hand, evidence regarding the formation of ettringite through the action of the sulfate solutions is less positive.

In the hydration products prior to sulfate attack, the Al_2O_3 appears to be distributed between ettringite, C-S-H, a hydrotalcite-type phase and a minor proportion of monosulfate, while the Fe_2O_3 appears to occur largely in a poorly crystalline hydrogarnet (13). Fully crystalline hydrogarnet phases high in iron or silicon or both are reported to be unreactive towards

sulfates (14–16). If it is assumed that only the Al_2O_3 in the monosulfate is available for reaction, the data in Fig. 3A could probably be explained almost wholly by the formation of gypsum. In contrast, the corresponding plot for a PC (Ref. 12, Fig. 6B) showed spots with compositions corresponding to high proportions of ettringite. At the other extreme, if it is assumed that all the Al_2O_3 and Fe_2O_3 react, the data in Fig. 3B could be explained by assuming the formation of gypsum and an Fe-substituted ettringite. The disappearance of the monosulfate, shown in Fig. 2C, provides indirect evidence that the content of ettringite in the SRPC paste increases to at least a small extent as a result of sulfate attack.

Stoichiometric calculations also indicate that much less ettringite is formed than with a typical PC. For the SRPC, calculations similar to those in Part II (13) suggest that not more than 1 % of Al_2O_3, together with a possible 1.6 % of Fe_2O_3, is available at 6 months for the formation of ettringite. The value for Al_2O_3 does not include some 0.6 % that is estimated to be present in ettringite at an age of 6 months in the absence of sulfate attack. For a typical PC, at least 3 % of Al_2O_3 and a possible 1.6 % of Fe_2O_3 are probably available. These estimates take into account the presence in the PC of aluminate phase and the fact that the ferrite in the PC is smaller in amount but likely to be more reactive.

Taken as a whole, the evidence suggests that some ettringite is formed, but that the amount is much less than with the PC studied in Part I (12). This conclusion contrasts with that of Heller and Ben-Yair (6), but is similar to those of Locher (7), Odler and Gasser (9) and Rasheeduzzafar and co-workers (10,11). Our results for the SRPC agree closely with those of the latter investigation. They are also broadly similar to those of Bonen and Cohen (17) for a cement that came near to meeting the ASTM Type V (sulfate-resisting) specification.

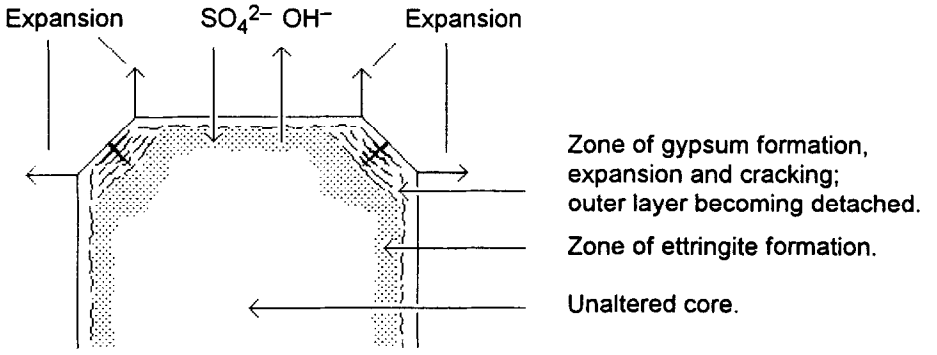

FIG. 7

Schematic representation of the microstructure of a section through a cube of a PC paste after immersion in a solution of Na_2SO_4, showing the suggested mechanism of expansion, based on the results of Gollop and Taylor (12). In varying degrees, the cracks are filled with gypsum, which is presumed to have been deposited in them by recrystallisation. For the SRPC paste studied in the present investigation, the microstructure and suggested mechanism of expansion are similar, but all the effects shown are less strongly developed. The diagram is not to scale.

Microstructure and Physical Effects

From the study of the reaction of a PC paste with Na_2SO_4 solution (12), the following sequence of reactions was proposed (Fig. 7). A reaction front advances into the paste, and its first effect is to produce ettringite. The presence of ettringite was inferred only from X-ray microanalyses, which corresponded to intimate mixtures of this phase with C-S-H. Subsequently, and therefore nearer to the external surface, gypsum is formed. The zone in which gypsum is formed is also one in which little or no calcium hydroxide is present and C-S-H is decalcified. Gypsum, like the ettringite, was present in close admixture with C-S-H, but some

also occurred in veins, which were sub parallel to the cube surfaces and especially abundant near the cube edges. Cracks were present, notably along the edges of the gypsum veins and running diagonally inwards from the cube edges. It was concluded that expansion occurred in the zone of gypsum formation, and that it was tending to cause the surface layer to become detached, thus forming cracks in which some of the gypsum recrystallized. Formation of both ettringite and gypsum requires Ca^{2+}, in addition to SO_4^{2-}. In the case of the ettringite, this was obtained by the dissolution of $Ca(OH)_2$, but in that of the gypsum, most was obtained by decalcification of the C-S-H. Cabrera and Plowman (18) and Wang (19) reported XRD examinations of the materials present at different depths in Portland cement pastes which had been subjected to attack by sodium sulfate solutions. The results indicated distributions of products similar to that described above.

The observation that cracking does not occur in the zone in which ettringite is formed, but nearer to the surface, appears to exclude the widely held hypothesis that expansion is a direct and immediate result of ettringite formation. Wang (19) considered that more damage was caused by the formation of gypsum than by that of ettringite. However, this hypothesis is difficult to reconcile with the many observations that expansion is related to C_3A content; also, we have found that cracking occurs in some pastes of slag cements in which little or no gypsum is formed (20). It is more likely that the immediate cause of the expansion is absorption of water by the cement gel, in which it replaces that used up in the formation of ettringite (12). This mechanism is closely derived from that suggested in 1952 by Thorvaldson (1) and has much in common with that suggested by Mehta (21).

For the SRPC studied in the present work, the sequence of reactions appears to be essentially the same as for the PC described above, but there are some important differences. The lesser degree of decalcification in the case of the SRPC can be explained by the smaller amount of Ca^{2+} that is required for the formation of ettringite. As a result, that used in forming gypsum is largely obtained at the expense of $Ca(OH)_2$. The decreased formation of ettringite and decreased decalcification of the C-S-H probably both contribute to the lower expansions and strength losses shown by typical SRPCs as compared with PCs. Because of the former effect, the forces tending to disrupt the paste are smaller, and because of the second, it is better able to withstand them.

All the above comments on the data obtained in the present investigation apply also to the cube immersed in $MgSO_4$ solution. In the latter case, as with the PC, a composite layer of brucite and gypsum is formed at the cube faces and there is substantial formation of magnesium silicate hydrate at the cube edges, resulting in major local damage to the microstructure. Because of these reactions, decalcification of the C-S-H is more marked than for the cube stored in Na_2SO_4 solution, though it is less marked than for the cube of the PC stored in $MgSO_4$ solution.

Two Types of External Sulfate Attack

Biczók (22) suggested that two types of external sulfate attack can occur. One, favoured by high C_3A content in the cement and by low sulfate concentration, was characterised by the formation of ettringite. The other, favoured by low C_3A content and by high sulfate concentration, was characterised by the formation of gypsum. The transition between the two types of attack was gradual, and both could occur simultaneously. Rasheeduzzafar and co-workers (10,11) came to a similar conclusion and considered that the formation of ettringite led to expansion but that the formation of gypsum led to loss of cohesion and softening of the cement matrix but to no more than a marginal degree of expansion. They attributed the loss of cohesion and softening more directly to incorporation of sulfate ions into the C-S-H. In contrast, Mehta (21) attributed it to decomposition of calcium hydroxide and C-S-H; this appears more probable.

These observations may account for the differing views in the literature (1,2) regarding the relative importance of ettringite formation and gypsum formation in external sulfate attack, and also for the apparent lack of correlation between the results of expansion tests and ones of

compressive strength or cohesion. Both the attack on the SRPC described in the present paper and that on the PC described in Part I (12) fall into the intermediate category in which both gypsum and ettringite are formed, with ettringite playing a relatively more important part in the case of the PC. No expansion data were obtained in the present investigation, but Lawrence (4,5) gave data for an SRPC (his $SRPC_2$; No. 3746) similar in composition to that studied here. The observed linear expansions, for 40 × 40 × 160 mm mortar prisms of w:c ratio 0.45 exposed to 0.3 mol l^{-1} $MgSO_4$ solution at 10°C for 3 years, were less than 0.1 mm more than those for control samples stored in water. Those for two PC's were significantly greater.

Conclusions

1. Reaction of a paste of an SRPC of w:c ratio 0.3 with 0.25 mol l^{-1} Na_2SO_4 solution followed the sequence previously reported for a PC under similar conditions, inward movement of a reaction front leading first to the formation of ettringite and later to that of gypsum. Very much less ettringite was formed than with the PC. Cracking, and, by implication, some degree of expansion, took place in the zone in which gypsum was formed. Cracking and loss of material at the cube edges were less severe with the SRPC than with the PC.

2. As with the PC, the ettringite formed through sulfate attack was intimately mixed with C-S-H on or below a micrometre scale. Gypsum was present in this form and also in a vein sub parallel to the surface. It is suggested that the vein resulted from recrystallisation in cracks produced by expansion.

3. The hydration products of an SRPC are low in Al_2O_3 relative to the other oxide components, and some of this Al_2O_3 is present as ettringite before attack begins. As a result, the increase in ettringite content resulting from sulfate attack is considerably less than in a PC paste. Because the formation of ettringite requires Ca^{2+} as well as SO_4^{2-}, decalcification of the C-S-H is also much reduced. The decreased ettringite formation lessens the forces tending to disrupt the paste, and the decreased decalcification renders the paste better able to withstand them.

4. Reaction with 0.25 mol l^{-1} $MgSO_4$ solution also appears to follow a similar course to that observed with the PC. The decalcification of the C-S-H is more marked than with Na_2SO_4. As with the PC, a composite layer of brucite and gypsum is formed on the cube faces and a poorly crystalline form of serpentine is formed at the cube edges. The reactions of the sulfate ions are essentially the same as in the case of Na_2SO_4.

5. The sequence of reactions described above was observed with pastes of low w:c ratio and relatively concentrated sulfate solutions. It does not necessarily occur under all conditions. Reports in the literature suggest that with weaker sulfate solutions, and also with PC's especially high in C_3A, reaction with Na_2SO_4 produces ettringite but little or no gypsum.

Acknowledgement

The authors wish to thank Blue Circle Industries PLC for permission to publish this study and for sponsoring RSG for an External Ph.D. course at Imperial College, University of London. The work forms part of the programme of research being carried out by RSG under the Public Institutions and Industrial Research Laboratories Scheme at Imperial College, where HFWT is a Visiting Professor. The authors are indebted to Dr G.K. Moir for his encouragement and advice. Similar thanks are due to Professor P.L. Pratt and Dr K.L. Scrivener, of the Department of Materials, Imperial College.

References

1. T. Thorvaldson, in Proceedings of the 3rd International Symposium on the Chemistry of Cement [London, 1952], p. 436. Cement and Concrete Association, London (1954).
2. I. Odler and I. Jawed, in Materials Science of Concrete II (J. Skalny and S. Mindess, Eds.), p. 221. American Ceramic Society, Westerville, Ohio, USA (1989).

3. J.J. Kollek and J.S. Lumley, in Proceedings of the 5th International Conference on the Durability of Building Materials and Components (J.M. Baker, P.J. Nixon, A.J. Majumdar and H. Davies, Eds.), p. 409 (1990).
4. C.D. Lawrence, Cem. Concr. Res. **22**, 1047 (1992).
5. C.D. Lawrence, Comparative Sulfate Resistance of Mortars Made with Different Binder Types. Publication C/14, British Cement Association, Crowthorne, Berks, UK (1993).
6. L. Heller and M. Ben-Yair, J. Appl. Chem. **14**, 20 (1964).
7. F.W. Locher, Zem.-Kalk-Gips **19**,395 (1966).
8. D. Dimic and S. Droljc, in 8th International Congress on the Chemistry of Cement [Rio de Janeiro], Vol. 5, p. 195. Abla Gráfica e Editora Ltda., Rio de Janeiro (1986).
9. I. Odler and M. Gasser, J. Am. Ceram. Soc. **71**, 1015 (1988).
10. Rasheeduzzafar, O. S. B. Al-Almoudi, S.N. Abduljauwad and M. Maslehuddin, J. Mater. Civil Engnrg. **6**, 201 (1994).
11. Rasheeduzzafar, F.H. Dakhil, A.S. Al-Gahtani, S.S. Al-Saadoun and M.A. Bader, ACI Mater. J. **87**, 114 (1990).
12. R.S. Gollop and H.F.W. Taylor, Cem. Concr. Res. **22**, 1027 (1992).
13. R.S. Gollop and H.F.W. Taylor, Cem. Concr. Res. **24**, 1347 (1994).
14. E.P. Flint and L.S. Wells, J. Res. Nat. Bur. Stands. **27**, 171 (1941).
15. H. zur Strassen, Zem.-Kalk-Gips **11**, 137 (1958).
16. B. Marchese and R. Sersale, in Proceedings of the 5th International Symposium on the Chemistry of Cement [Tokyo, 1968], Vol. 2, p. 133. Cement Association of Japan, Tokyo (1969).
17. D. Bonen and M.D. Cohen, Cem. Concr. Res. **22**, 169, 707 (1992).
18. J.G. Cabrera and C. Plowman, Adv. Cem. Res. **1**, 171 (1988).
19. J.G. Wang, Cem. Concr. Res. **24**, 735 (1994).
20. R.S. Gollop and H.F.W. Taylor, in preparation.
21. P.K. Mehta, in Materials Science of Concrete III (J. Skalny, Ed.), p. 105. American Ceramic Society, Westerville, Ohio, USA (1992).
22. I. Biczók, Concrete Corrosion, Concrete Protection, 8th Ed., p.192 et seq. Akadémiai Kiadó, Budapest (1972).